

Electronic Supplementary Information

Vacuum-ultraviolet irradiation of pyridine:acetylene ices relevant to Titan astrochemistry

Larissa Lopes Cavalcante,^a Ellen C. Czaplinski,^b Helen E. Maynard-Casely,^c Morgan Cable,^b Naila Chaouche,^a Robert Hodyss,^b Courtney Ennis^{a,d*}

^a *Department of Chemistry, University of Otago, Dunedin 9054, New Zealand*

^b *Jet Propulsion Laboratory, California Institute of Technology, Pasadena, California 91109, United States*

^c *Australian Centre for Neutron Scattering, ANSTO, Kirrawee, New South Wales 2232, Australia*

^d *MacDiarmid Institute for Advanced Materials and Nanotechnology, Wellington 6140, New Zealand*

* *courtney.ennis@otago.ac.nz*

Table of Contents

Section 1: VUV calibration procedure

Section 2: Supporting tables and figures

Section 3: C₂H₂ periodic-DFT (CRYSTAL17) output: geometry, frequency, cell energies

Section 4: C₅H₅N periodic-DFT (CRYSTAL17) output: geometry, frequency, cell energies

Section 5: C₅H₅N-C₂H₂ co-crystal periodic-DFT (CRYSTAL17) output: geometry, frequency, cell energies

Section 1: VUV Calibration procedure

The VUV light source calibration procedure was followed according to the previously described method¹. Briefly, the photoconversion of solid O₂ ice to ozone was monitored using FTIR transmission spectroscopy. The intensity of the strong O₃ ν₃ band at 1040 cm⁻¹ ($A = 1.4 \times 10^{-17}$ cm molecule⁻¹) was measured over time following a linear response before IR signal saturation. The flux of VUV photons irradiating the 10 mm radius KBr substrate was calculated to be of the order of $\sim 10^{12}$ photons cm⁻² s⁻¹.

Section 2: Supporting tables and figures

Table S1. IR vibrational bands and respective assignments for the C₅H₅N:C₂H₂ co-crystal and pure phases.

C ₅ H ₅ N				C ₂ H ₂		Co-crystal	Δν between pure and co- crystal	Vibrational modes
Hudson et al. 2022		This work		Hudson et al. 2014	This work	This work		
Amorphous 10 K	Crystalline 130 K	Crystalline 130 K	Amorphous 110 K	Crystalline 15 K	Crystalline 70 K	Crystalline 110 K		
				3226 (b)	3243 (sh)/3227 (vs)	3233	-6	ν ₃ (νCH) ^{a,b}
						3178 3143 3085		co-crystal bands
3078	3078	3078	3076			3080	-4	ν ₁₁ (νCH) ^{c,d}
3051	3055	3054	3050			3053	-3	ν ₂ (νCH) ^{c,d}
	3030	3029	3032			3032	0	ν ₃ (νCH) ^{c,d}
3026	3019	3021	3025			3026	-1	ν ₁₂ (νCH) ^{c,d}
3002						3004	-2	
2989	2996	2996;2987	2995			2990	-3	ν ₁₄₊₄ ^c
1598	1599	1598	1597			1603	-6	ν ₉₊₁₀ ^c
						1598	-1	
1582	1580	1580	1581			1584	-3	ν ₄ (ν ring +δCH) ^{c,d}
						1582	-1	
1572	1571	1570	1571			1571	0	ν ₁₃ (ν ring +δCH) ^{c,d}
1483	1480	1480	1483			1484	-1	ν ₅ (ν ring +δCH) ^{c,d}
1438	1435	1432	1437			1438	-1	ν ₁₄ (ν ring) ^{c,d}

	1354	1382; 1355					ν_{15} (v ring + δ CH) ^{c,d}
			1228		1229	-1	
1218		1211	1217		1217	0	ν_{16} (v ring + δ CH) ^{c,d}
					1212	1	
		1203	1206		1204	2	ν_6 (v ring + δ CH) ^{c,d}
1146	1142	1141	1146		1146	0	ν_{17} (v ring + δ CH) ^{c,d}
1068	1065	1065	1067		1067	0	ν_7 (v ring + δ CH) ^{c,d}
	-	1053	1055		1055	0	ν_{18} (v ring + δ CH) ^{c,d}
1031	1031	1031	1030		1030	0	ν_8 (v ring) ^{c,d}
991	991	990	990		992	-2	ν_9 (γ CH) ^{c,d}
		954	979				ν_{20} (v ring) ^{c,d}
		949	945		948	-3	ν_{23} (γ CH) ^{c,d}
		889					ν_{24} (γ CH) ^{c,d}
					838		
					820		co-crystal bands
					805		
					788		
				770	769		
				761	759		ν_5 (δ CH) ^{a,b}
750	754	754	751		750	1	ν_{25} (γ CH + τ ring) ^{c,d}
				745	745		ν_5 (δ CH) ^{a,b}
705	707	705	705		704	1	ν_{26} (γ CH + τ ring) ^{c,d}
605	604	603	604		605	-1	ν_{10} (v ring) ^{c,d}

Positive value of $\Delta\nu$ indicates a redshift; a negative value of $\Delta\nu$ indicates a blueshift. ν , stretching; ν ring, in-plane ring deformation; δ , bending; γ , wagging; τ , out-of-plane ring deformation. ^aHudson et al., 2014²; ^bBottger & Eggers, 1964³; ^cCastellucci et al., 1969⁴; ^dUrena et al., 2003⁵.

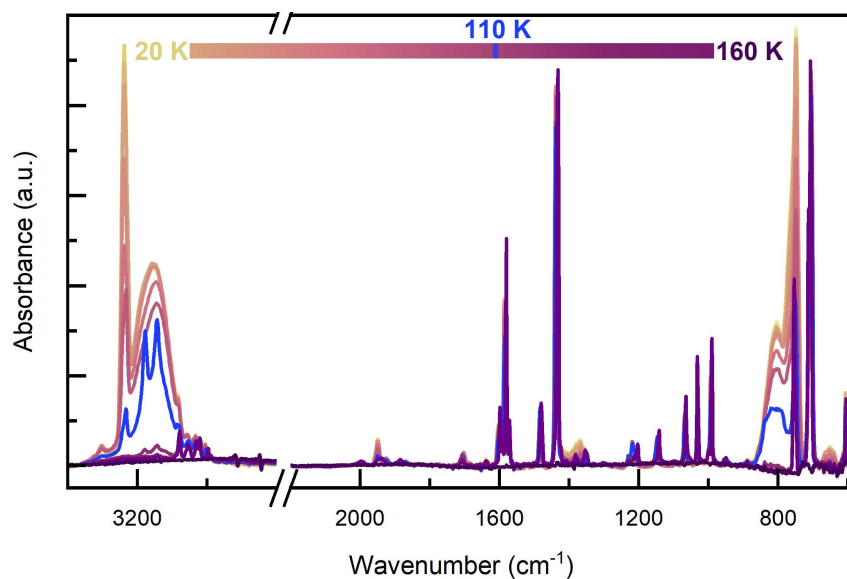


Figure S1. Temperature ramp from 20 to 160 K showing the progressive co-crystal formation at 110 K, with 10 K steps between each spectrum. At base temperature, the spectrum is characterized by the presence of a broad band in the CH stretch region, centered at 3152 cm^{-1} , and a shoulder around 810 cm^{-1} developing to the 889 cm^{-1} CH wagging mode of $\text{C}_5\text{H}_5\text{N}$, both indicating an interaction between acetylene and pyridine. At 110 K, co-crystallization is observed as indicated by the broad band CH band becoming resolved and splitting into two bands at 3178 and 3142 cm^{-1} , corresponding to coupled CH stretching modes of pyridine and acetylene. The shoulder at 810 cm^{-1} becomes more resolved into a structured broad band, corresponding to the coupled bending modes of acetylene and pyridine within the co-crystal.

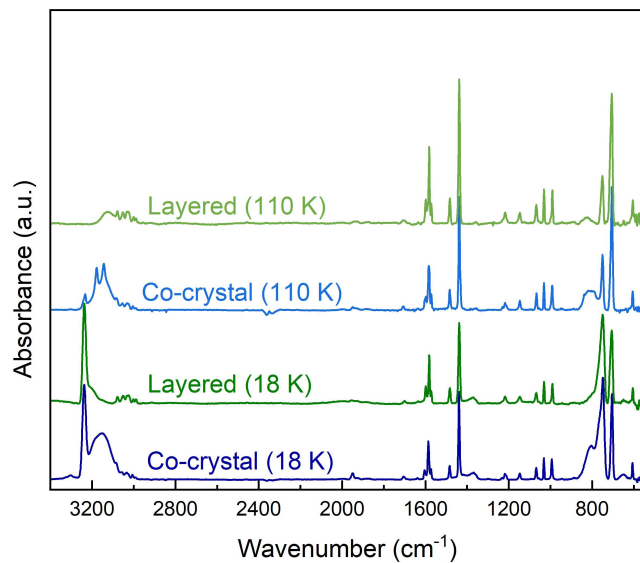


Figure S2. Stack plot of co-crystal (blue) and layered ices (green) between pyridine and acetylene. For the layered ice, the acetylene was deposited on top of pyridine, following the condensation profile of gases in Titan's atmosphere⁶, and assuming pyridine condensation at a similar altitude to benzene. The absence of the strong features that characterize the co-crystal formation in the spectrum for the layered ice indicates poor interaction between the two species, being restricted to the interface between the two ice layers. At 110 K, the persistence of broad bands at 3125 and 824 cm⁻¹ indicates that the remaining acetylene molecules in the ice are interacting with pyridine but without a preferred orientation, i.e. co-crystal formation.

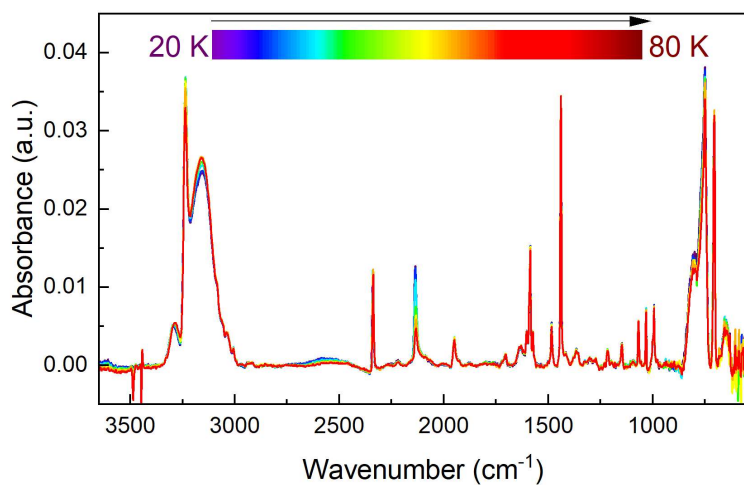


Figure S3. Infrared spectra recorded during temperature ramp between 20 and 80 K after irradiation of the mixed ice at 18 K.

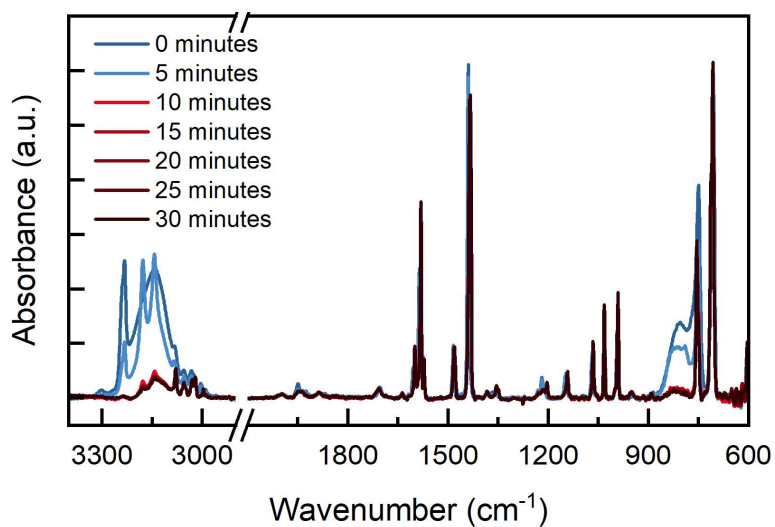


Figure S4. Stability of the co-crystal after formation at 110 K. Within 30 minutes, the bands associated with the co-crystal formation considerably deplete, resulting from the instability caused by the desorption of acetylene at those temperatures and under vacuum.

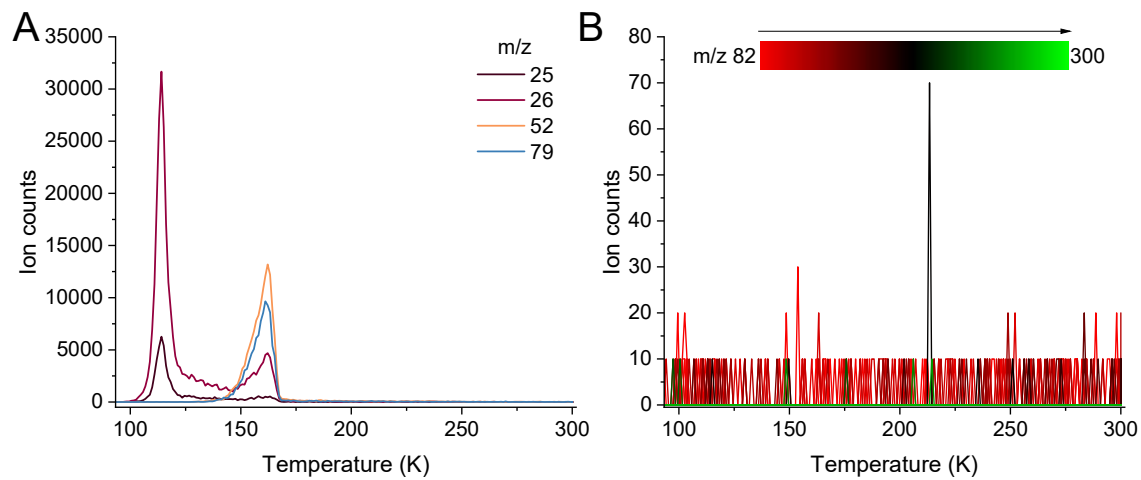


Figure S5: Ion counts for the co-crystal irradiated at 90 K. (A) Parent molecules: m/z 25 and 26 (C_2H^+ and C_2H_2^+); m/z 52 and 79 (C_4H_4^+ and $\text{C}_5\text{H}_5\text{N}^+$). (B) Ion counts for masses between m/z 82 and 300. Occasional spikes were considered noise.

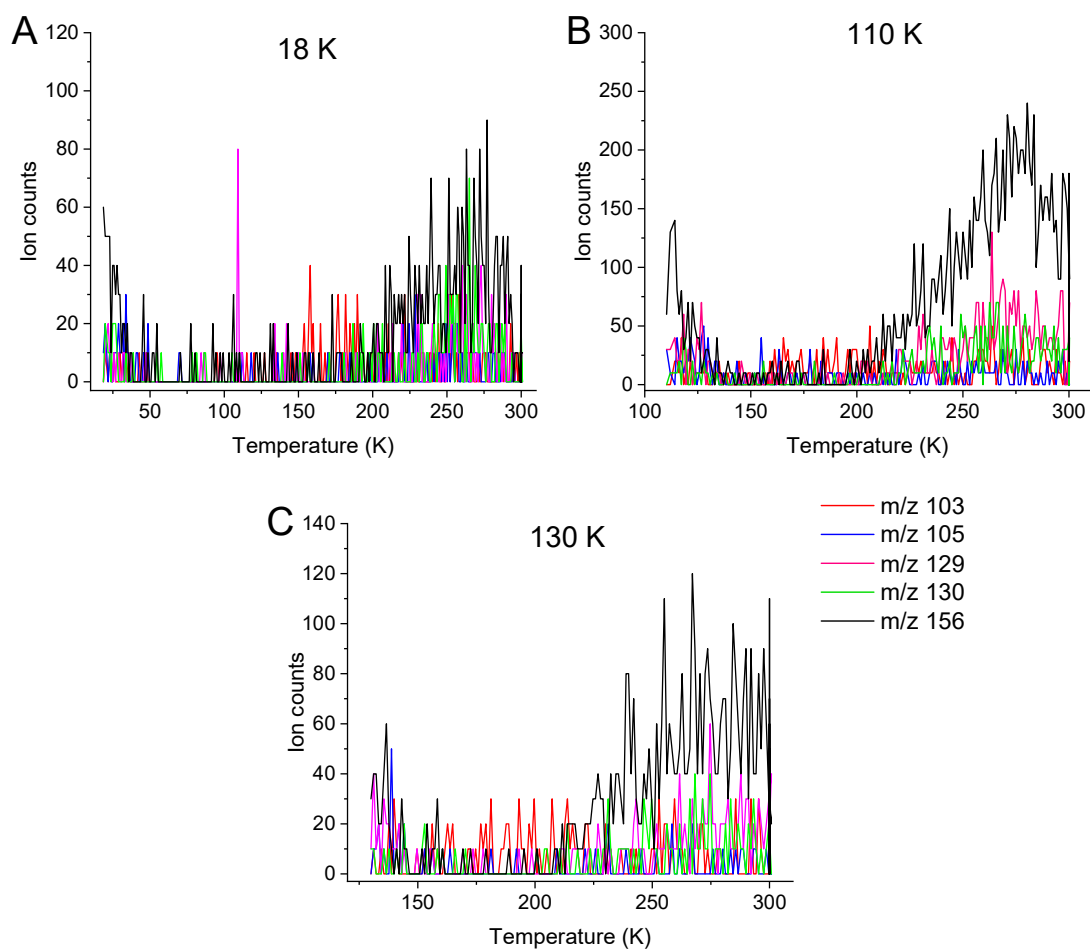


Figure S6: Ion counts for target ions evaluated throughout by TPD until 300 K for the pure pyridine ices irradiated for 48 h at: (A) 18 K, (B) 110 K and (C) 130 K. Overall, the most abundant specie has m/z 156, indicating the formation of bipyridine structures, and desorbs from ~200 K. Only trace levels of m/z 103, 129 and 130 detected and an absence of m/z 105 above the noise threshold.

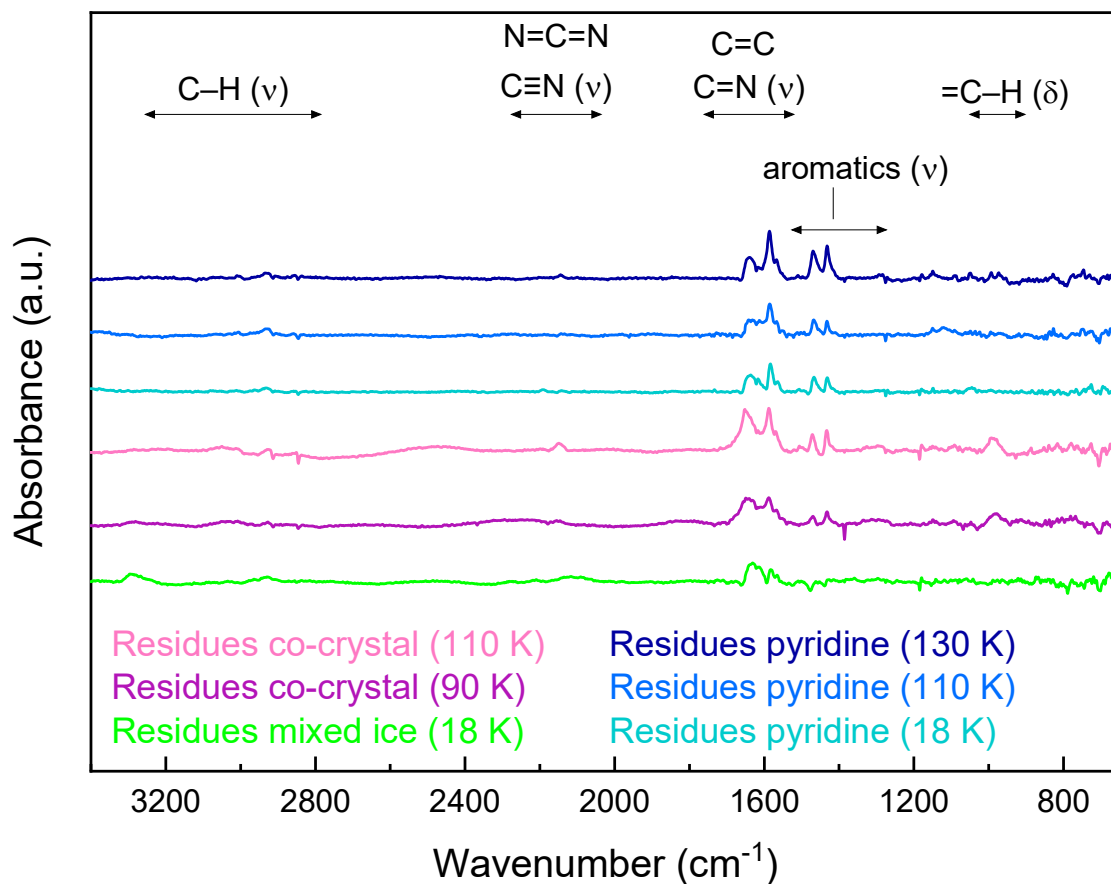


Figure S7. Stacked spectra of the non-volatile residues formed after 48 h irradiation of the pure $\text{C}_5\text{H}_5\text{N}$ and mixed ices between $\text{C}_5\text{H}_5\text{N}$ and C_2H_2 , followed by temperature ramp to 300 K. The residues formed within the co-crystals irradiated at 90 (purple) and 110 K (pink) are the same, also showing strong similarities with the mixed ice irradiated at 18 K (green) and pure $\text{C}_5\text{H}_5\text{N}$ ices irradiated at 18 (cyan), 110 (light blue) and 130 K (dark blue). The region of the vibrational modes was assigned based on previous studies⁷. ν = stretching; δ = bending.

References

1. P. A. Gerakines, M. H. Moore and R. L. Hudson, *Astronomy and Astrophysics*, 2000, **357**, 793-800.
2. R. L. Hudson, R. F. Ferrante and M. H. Moore, *Icarus*, 2014, **228**, 276-287.
3. G. L. Bottger and D. F. Eggers, *The Journal of Chemical Physics*, 1964, **40**, 2010-2017.
4. E. Castellucci, G. Sbrana and F. D. Verderame, *The Journal of Chemical Physics*, 1969, **51**, 3762-3770.
5. F. P. Ureña, M. F. Gómez, J. J. L. González and E. M. n. Torres, *Spectrochimica Acta Part A: Molecular and Biomolecular Spectroscopy*, 2003, **59**, 14.
6. E. L. Barth, *Planetary and Space Science*, 2017, **137**, 20-31.
7. E. Hirai, Y. Sekine, N. Zhang, N. Noda, S. Tan, Y. Takahashi and H. Kagi, *Geophysical Research Letters*, 2023, **50**.